

Extreme sea wave modelling: Application to rogue waves

Christian Kharif

Institut de Recherche sur les Phénomènes Hors Equilibre (IRPHE)
Marseille, France

Collaborators:

Jean-Paul Giovanangeli (IRPHE), Olivier Kimmoun (IRPHE),
Efim Pelinovsky (IAP) and Julien Touboul (LSEET)

Rogue Waves in the presence of wind

Outline

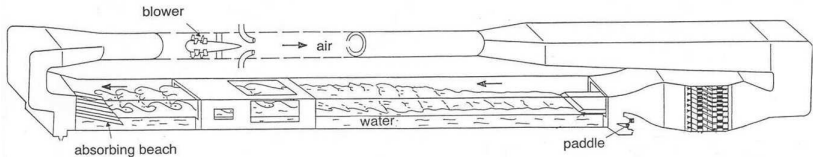
- ▶ Experiments in deep water
- ▶ Modelling
 - ▶ Wind models
 - ▶ The Miles mechanism
 - ▶ The modified Jeffreys' mechanism
 - ▶ Numerical simulations of rogue waves
 - ▶ Numerical method
 - ▶ In deep water
 - ▶ Infinite depth

- ▶ Based on *in situ* data and numerical simulations Waseda *et al* (2011) invoke that local winds may influence the rogue wave occurrence

I. Experiments in deep water

The dispersive focusing

- ▶ **Water tank dimensions:** 40m long, 2.6m wide, 1m deep
- ▶ **Wind tunnel dimensions:** 40m long, 3.2m wide, 1.6m high
- ▶ **Paddle:** 0.5Hz - 2Hz (regular or random waves)



The Large Air-Sea Interaction Facility of IRPHE.

- ▶ What is the frequency to impose to a wave-maker located at $x = 0$ to generate a big wave at $x = x_f$ and $t = t_f$?
- ▶ In infinite depth case the paddle frequency to impose is

$$\omega_0(\tau) = \frac{1}{2} \frac{g}{x_f} (t_f - \tau)$$

$$f(\tau) = \frac{g}{4\pi} \frac{t_f - \tau}{x_f}$$

$$\tau = 0, \quad f = f_{\max}$$

$$\tau = T, \quad f = f_{\min}$$

$$x_f = \frac{gT}{4\pi(f_{\max} - f_{\min})}, \quad t_f = \frac{4\pi f_{\max} x_f}{g}$$

► Paddle parameters

$$f_{\max} = 1.3\text{Hz}$$

$$f_{\min} = 0.8\text{Hz}$$

$$T = 10\text{s}$$



$$x_f \approx 16\text{m}$$

$$t_f \approx 26\text{s}$$

► Wind speed range

$$U = 0, 4, 6, 8\text{m/s}$$

- The upstream wave gauge is located at a fixed distance of 1 m from the upstream beach
- The downstream gauge is moved at different fetches from 6 m to 35 m from the upstream beach

Water wave parameters

$$(ak)_{\min} \approx 0.075$$

$$(ak)_{\max} \approx 0.20$$

$$(kh)_{\min} \approx 2.6$$

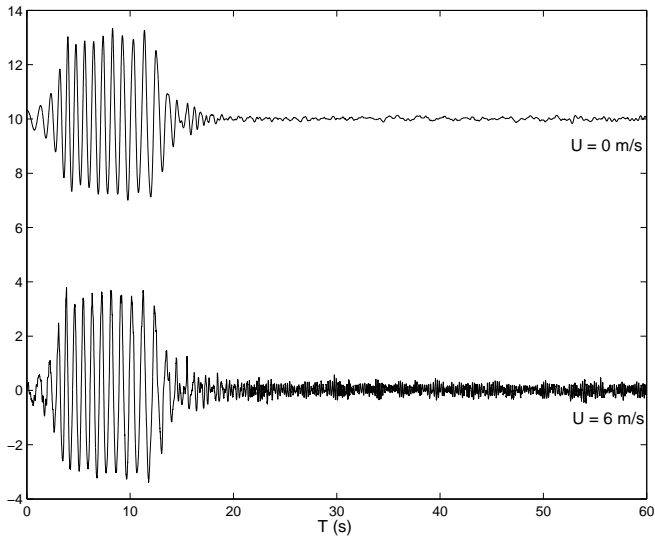
$$(kh)_{\max} \approx 6.8$$

$$(k)_{\min} \approx 2.6m^{-1}$$

$$(k)_{\max} \approx 6.8m^{-1}$$

$$\lambda_{\min} \approx 0.9m$$

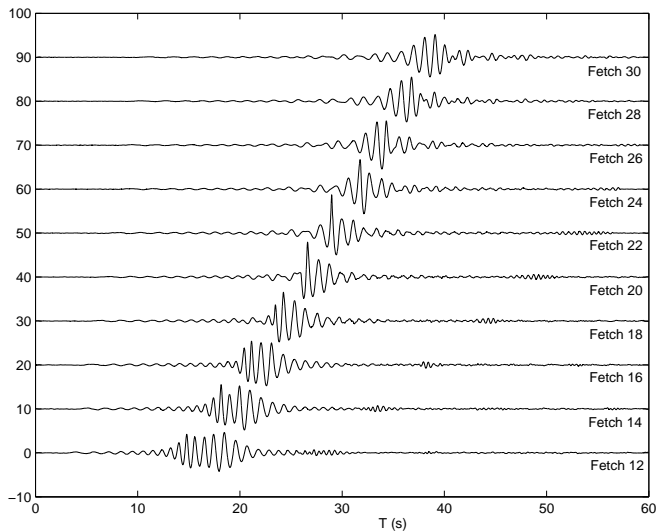
$$\lambda_{\max} \approx 6.8m$$



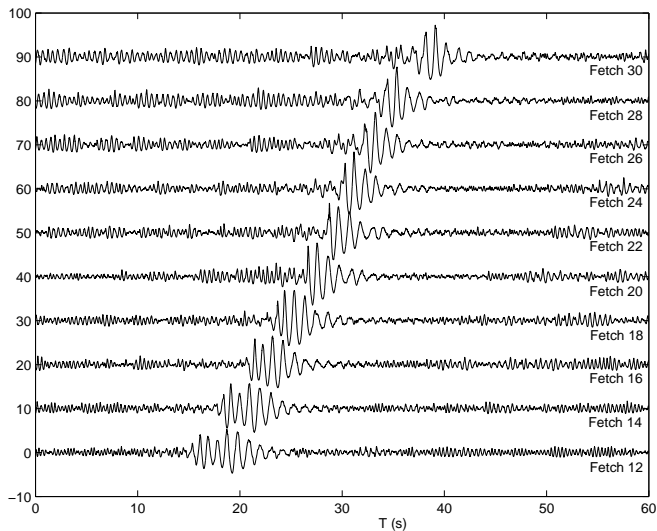
Surface elevation (in *cm*) at fetch $x = 1m$, for wind speeds $U = 0$ and $6m/s$: Mean wave height $H_{ref} = H(1, U) = 6cm$

Wind Velocity (m/s)	$\sqrt{\langle \eta^2 \rangle}$ (cm)
0	1.88
4	1.88
5	1.87
6	1.88
8	1.87
10	1.88

The r.m.s. elevation for different values of the wind velocity at
fetch $1m$



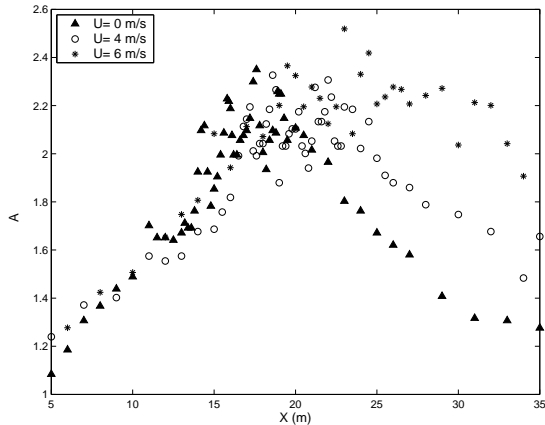
Surface elevation (in *cm*) at several fetches (in *m*), for wind speed
 $U = 0 \text{ m/s}$, as a function of time



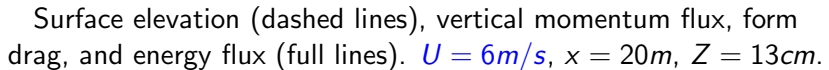
Surface elevation (in *cm*) at several fetches (in *m*), for wind speed
 $U = 6\text{ m/s}$, as a function of time

Amplification factor

$$A(x, U) = \frac{H_{\max}}{H_{\text{ref}}}, \quad H_{\text{ref}} = H(1, U) = 6\text{cm}$$



Amplification factor $A(x, U)$ as a function of the fetch, for several values of the wind speed



Preliminary conclusions

- ▶ The dispersive focusing is a **robust mechanism** (the wind does not cancel the focusing process)
 - ▶ The wind **increases the duration of the rogue wave** event
 - ▶ The **amplification factor increases slightly** with wind velocity
 - ▶ The wind shifts downstream the focus point
 - ▶ The air-sea fluxes are strongly enhanced in the presence of steep wave groups
-
- ▶ For more details see Kharif *et al*, JFM, 594, 2008

II. Modelling

The dispersive focusing

II.1 Wind models

- ▶ **The question is:** Which simple wind modelling to use to describe the increase of the lifetime of the steep wave group?

- ▶ **The Miles' mechanism**: A linear theory of wind wave generation (Miles 1957, 1993, 1996)

Hypothesis: Air and Water are inviscid, incompressible fluids and the motion is irrotational in water

The transfer of energy from a shear flow $U(z)$ to a surface wave of wavenumber k and phase velocity c is associated with a singularity at the critical layer $U(z = z_c) = c$ (parallel shear flow instability).

$$\frac{\partial \bar{E}}{\partial t} = -\rho_a c \pi \left(\frac{d^2 U}{dz^2}(z_c) / k \left| \frac{dU}{dz}(z_c) \right| \right) \overline{w^2(z_c)} \quad (1)$$

where E is the surface wave energy, ρ_a is air density and $w(z_c)$ the vertical velocity at $z = z_c$ (overbar means an average over x)

Writing $\partial E / \partial t = \gamma E$, we introduce the Miles coefficient β such as

$$\gamma = \frac{\rho_a}{\rho_w} k c \beta \left(\frac{U_1}{c} \right)^2 = s \omega \beta \left(\frac{U_1}{c} \right)^2 \quad (2)$$

where $s = \frac{\rho_a}{\rho_w}$, $\omega = kc$, the velocity U_1 is related to the friction velocity, u_* , of wind over the water waves (for a logarithmic profile $U_1 = u_*/\kappa$ where κ is the von Karman's constant), and β is

$$\beta = -\pi \frac{\frac{d^2 U}{dz^2}(z_c)}{k \left| \frac{dU}{dz}(z_c) \right|} \frac{\overline{w^2(z_c)}}{U_1^2 \left(\frac{\partial h_0}{\partial x} \right)^2} \quad (3)$$

The interface equation is $z = a \cos kx = h_0(x)$

More physically, when introducing $\eta(x, t) = ae^{ik(x-ct)}$, the surface elevation and $p_a = (\alpha + i\beta)\rho_a U_1^2 k\eta$, the pressure at the interface, into the linearized surface wave equations \Rightarrow Exponential growth rate γ of the energy and γ_a of the amplitude

$$\gamma = kcs\beta\left(\frac{U_1}{c}\right)^2 = \omega s\beta\left(\frac{U_1}{c}\right)^2 \quad (4)$$

$$\gamma_a = \frac{1}{2}\omega s\beta\left(\frac{U_1}{c}\right)^2 \quad (5)$$

- ▶ **The sheltering mechanism:** A wave growth mechanism
- ▶ *The non-separated sheltering:* (Belcher and Hunt, 1993)
Thickening of the BL on the leeward side of the crest \Rightarrow pressure asymmetry
- ▶ *The separated sheltering or Jeffreys' mechanism:* (Jeffreys, 1925) For steep waves \Rightarrow mean flow separation (Banner and Melville, 1976)

Jeffreys (1925) suggested that the phase shift between the surface elevation and the pressure is due to flow separation occurrence

$$p_a = \rho_a C_{sh} (U_\infty - c)^2 \frac{\partial \eta}{\partial x} \quad (6)$$

ρ_a , air density; C_{sh} , sheltering coefficient; U_∞ , wind velocity; and c , wave phase velocity

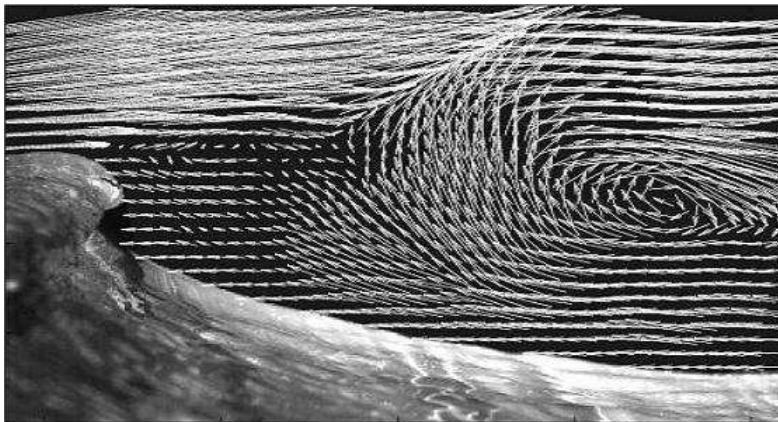
The wave energy growth rate

$$\gamma = s\omega C_{sh} \left(\frac{U_\infty - c}{c} \right)^2 \quad (7)$$

The wave amplitude growth rate

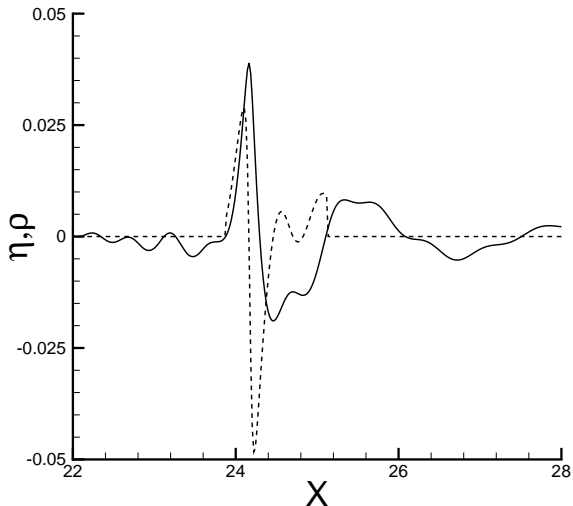
$$\gamma_a = s \frac{1}{2} \omega C_{sh} \left(\frac{U_\infty - c}{c} \right)^2 \quad (8)$$

Air flow separation observed by PIV (Reul *et al*, 1999)



- ▶ **The modified Jeffreys' sheltering mechanism:** Unlike Jeffreys we assume that air flow separation occurs only above very steep crests of wave steepness larger than a critical threshold value

$$\begin{cases} p_a(x) = 0 & \text{if } |\partial\eta/\partial x|_{\max} < |\partial\eta/\partial x|_c \\ p_a(x) = \rho_a C_{sh} (U - c)^2 \frac{\partial\eta}{\partial x}(x) & \text{if } |\partial\eta/\partial x|_{\max} \geq |\partial\eta/\partial x|_c \end{cases}$$



Pressure distribution (dashed line) on the interface (solid line)

Theoretical approach

Let $\eta(x, t) = \epsilon A(\xi, \tau) \exp(k_0 x - \omega_0 t)$ be the surface elevation

- ▶ ϵA : complex amplitude
- ▶ ϵ : small parameter
- ▶ $\xi = \epsilon^2 k_0 x$
- ▶ $\tau = \epsilon \omega_0 (t - x/c_g)$

Introducing the dimensionless amplitude $a(\xi, \tau) = k_0 A(\xi, \tau)$, the spatial NLS equation that is more suitable than the temporal version to model wave evolution in a tank writes

$$i\partial_\xi a - \partial_{\tau\tau} a - |a|^2 a = 0 \quad (9)$$

In the presence of a forcing term due the Miles' mechanism

$$i\partial_{\xi}a - \partial_{\tau\tau}a - |a|^2a = i\delta_a a \quad (10)$$

with

$$\delta_a = 2\frac{\gamma_a}{\omega} = s\beta\left(\frac{U_1}{c}\right)^2$$

and for a logarithmic profile

$$\delta_a = \frac{s\beta}{\kappa}\left(\frac{u_*}{c}\right)^2$$

First, let us consider the linear version of f-NLS equation (10) to describe the focusing of a linear wave group under wind action

$$i\partial_{\xi}a = \partial_{\tau\tau}a + i\delta_a a \quad (11)$$

Introducing $a(\xi, \tau) = b(\xi, \tau) \exp(\delta_a \xi)$

$$i\partial_{\xi}b = \partial_{\tau\tau}b \quad (12)$$

For the boundary value $b(0, \tau) = b_0 \exp(-\Omega_0^2 \tau^2)$, the Schrödinger equation (13) admits the following exact solution

$$b(\xi, \tau) = \frac{b_0}{\sqrt{1 - 4i\Omega_0^2 \xi}} \exp\left(-\frac{\Omega_0^2 \tau^2}{1 - 4i\Omega_0^2 \xi}\right) \quad (13)$$

and

$$a(\xi, \tau) = |a(\xi, \tau)| \exp(-i\Phi(\xi, \tau)) \quad (14)$$

with

$$|a(\xi, \tau)| = \frac{b_0}{(1 + 16\Omega_0^4 \xi^2)^{1/4}} \exp(-\Omega_0^2 \tau^2 / (1 + 16\Omega_0^4 \xi^2)) \exp(\delta_a \xi) \quad (15)$$

and

$$\Phi(\xi, \tau) = -\frac{4\Omega_0^4 \tau^2 \xi}{1 + 16\Omega_0^4 \xi^2} + \frac{1}{2} \arctan(4\Omega_0^2 \xi) \quad (16)$$

► No wind: $\delta_a = 0$

Wave packet of Gaussian envelope linearly modulated in frequency. Low frequency oscillations emitted in front of the high frequency oscillations. Due to dispersion the maximum of amplitude decreases as the group propagates: The wave packet is stretched

Let the wave group propagates and then use the transformation $\xi \rightarrow -\xi$, in order to have high frequency oscillations located in front of low frequency oscillations: the wave packet is compressed

Let L be the focusing distance: the amplification factor of the envelope amplitude at location ξ is

$$\frac{|a(\xi, \tau)|_{mx}}{|a(L, \tau)|_{mx}} = \left[\frac{1 + 16\Omega^4 L^2}{1 + 16\Omega^4 \xi^2} \right]^{1/4} \quad (17)$$

To have the wave maker located at $\xi = -L$ and the focusing point located at $\xi = 0$, we introduce the dimensionless variable

$$Z = 1 + \xi/L$$

The envelope amplification factor is

$$\mathcal{A}(Z) = \frac{|a(Z, \tau)|_{mx}}{|a(0, \tau)|_{mx}} = \left[\frac{1 + 16\Omega_0^4 L^2}{1 + 16\Omega_0^4 L^2 (Z - 1)^2} \right]^{1/4} \quad (18)$$

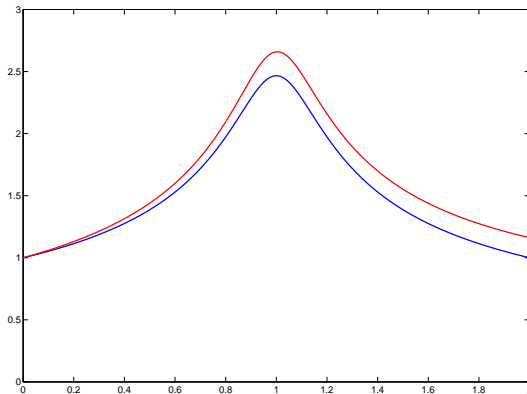
- ▶ $Z = 0 \rightarrow$ location of the wave maker
- ▶ $Z = 1 \rightarrow$ location of the focusing

- ▶ **With wind:** $\delta_a > 0$

$$\mathcal{A}(Z) = \left[\frac{1 + 16\Omega_0^4 L^2}{1 + 16\Omega_0^4 L^2 (Z1)^2} \right]^{1/4} \exp(\delta_a LZ) \quad (19)$$

- ▶ The presence of the wind breaks the symmetry between the focusing and defocusing stages.
- ▶ Three effects: The lifetime of the rogue event and amplification factor are increased, and the focusing point corresponding to the maximum of amplification is shifted downwind.

Normalized envelope amplification $\mathcal{A}(Z)$

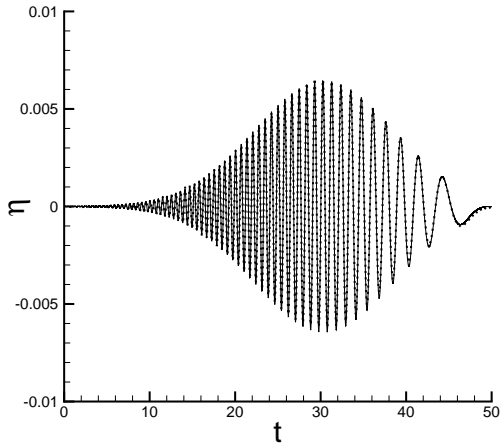


Blue line: without wind and red line: with wind

Numerical approach:

- ▶ Fully nonlinear water wave equations
- ▶ inviscid and incompressible fluid
- ▶ $2D$ and irrotational motion
- ▶ Numerical treatment: Boundary Integral Equation Method (BIEM) and a MEL marching scheme

Surface elevation as a function of time at the wave maker (case 4)



Solid line: analytical solution with $b_0 = 0.30$, $\Omega_0 = 0.30$, $\omega_0 = 2\pi$

Dotted line: obtained iteratively for the numerical wave tank

(The focusing occurs at $15m$)

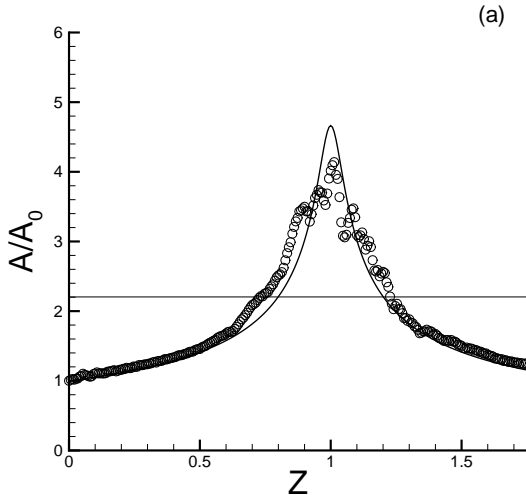
Parameters for the pressure term due to Miles' mechanism

$$\kappa = 0.4, \quad u_*/c = 0.2 \Rightarrow \beta = 3 \text{ (see Miles (1996))}$$

For numerical simulations the amplification factor is given by

$$\mathcal{A}(z) = \frac{\max\{\eta(z, t)\}}{\max\{\eta(0, t)\}} \quad (20)$$

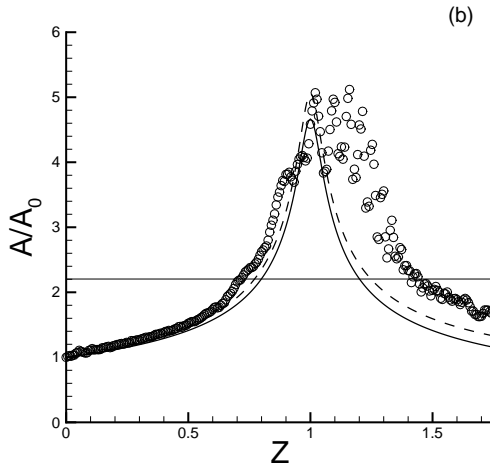
Amplification factor \mathcal{A} for a transient group, without wind



Solid line: analytical solution with $\delta_a = 0$

Circles: numerical solution without wind

Amplification factor \mathcal{A} in the presence of Miles' mechanism

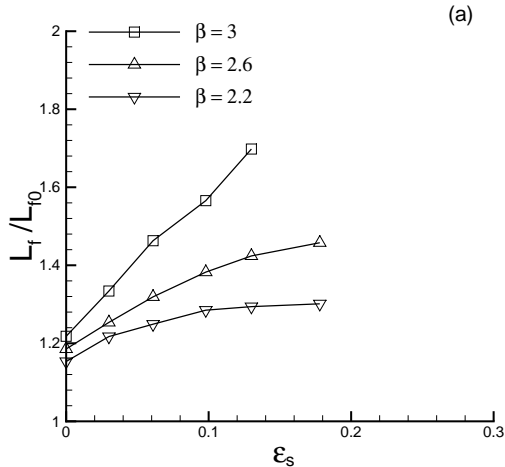


Solid line: analytical solution with $\delta_a = 0$

Dashed line: analytical solution with wind

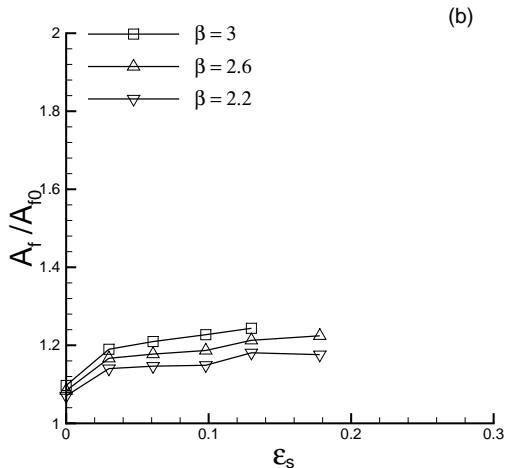
Circles: numerical solution without wind

Length of existence of steep wave events under Miles' mechanism



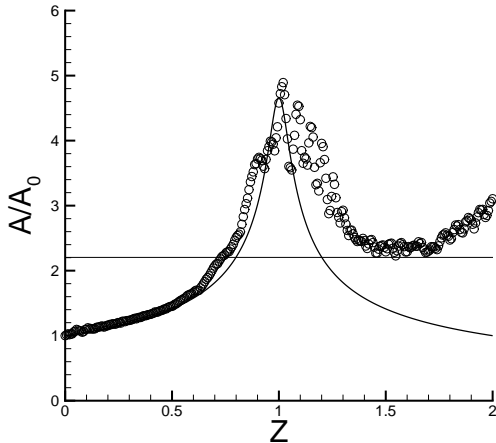
L_f and L_{f0} : lengths of existence with and without wind respect.
 ϵ_s : maximum local slope from numerical simulations without wind

Maximal amplitude in the wave group under Miles' mechanism



A_f and A_{f0} : Maximal amplitudes with and without wind respect.
 ϵ_s : maximum local slope from numerical simulations without wind

Amplification factor \mathcal{A} for a transient group under Jeffreys' mechanism (case 7)



Solid line: analytical solution with $\delta_a = 0$

Circles: simulation with $C_{sh} = 0.5$, $|\partial\eta/\partial x|_c = 0.6|\partial\eta/\partial x|_{\max}$

Conclusion on wind modelling

The linear theory

- ▶ The Miles' mechanism of wave amplification



- ▶ (i) a weak amplification of the wave envelope
- ▶ (ii) a weak asymmetry between focusing and defocusing stages resulting in a weak increase of the persistence of highest waves of the group.

The nonlinear approach

- ▶ The tendency (i) of the linear theory is confirmed: water wave nonlinearity increases the amplification factor \mathcal{A} slightly
- ▶ The tendency (ii) of the linear theory is strongly amplified: a strong asymmetry between focusing and defocusing is observed. The persistence of the highest waves of the group increases with water wave nonlinearity, ε_s , and wind input, β
- ▶ Nevertheless, the persistence of nonlinear wave events (i.e. L_f) due to the Miles' mechanism is underestimated when compared with experimental results.
- ▶ The Modified Jeffreys sheltering mechanism as wind model above steep waves provides results in agreement with experiments of Kharif *et al* (2008)
- ▶ For more details see Touboul *et al*, NPG, 15, 2008

II.2 Numerical simulations of rogue waves

Numerical approach:

The fully nonlinear equations

- ▶ inviscid and incompressible fluid
- ▶ 2D and irrotational motion

$$\Delta\Phi = 0, \quad \text{in} \quad \Omega, \quad (21)$$

$$\frac{D\mathbf{r}}{Dt} = \nabla\Phi, \quad \text{on} \quad \partial\Omega_{FS} \quad (22)$$

$$\frac{D\Phi}{Dt} = \frac{1}{2}\nabla\Phi \cdot \nabla\Phi - g\eta - \frac{p_a}{\rho_w}, \quad \text{on} \quad \partial\Omega_{FS} \quad (23)$$

$$\nabla\Phi \cdot \mathbf{n} = \mathbf{v} \cdot \mathbf{n}, \quad \text{on} \quad \partial\Omega_{SB} \quad (24)$$

- ▶ $\Phi(x, z, t)$ is the velocity potential, $D/Dt = \partial/\partial t + \nabla\Phi \cdot \nabla$
- ▶ \mathbf{r} is the position vector on the free surface
- ▶ \mathbf{v} is the velocity of the solid boundaries
- ▶ \mathbf{n} the unit normal vector

The Boundary Integral Equation Method (BIEM)

The Laplace equation (1) is transformed into a BIE by means of the Green's second identity

$$\int_{\partial\Omega} \Phi(P) \frac{\partial G}{\partial n}(P, Q) ds - \int_{\partial\Omega} \frac{\partial \Phi}{\partial n}(P) G(P, Q) ds = \alpha(Q) \Phi(Q), \quad (25)$$

- ▶ P and Q denote two points of the domain Ω
- ▶ G is the Green function $G(P, Q) = \ln(|\mathbf{PQ}|)$
- ▶ $\alpha(Q)$ the inner angle between two consecutive panels is defined as follows

$$\alpha(Q) = \begin{cases} 0 & \text{when } Q \text{ is outside } \Omega \\ \alpha & \text{when } Q \text{ is on } \partial\Omega \\ 2\pi & \text{when } Q \text{ is inside } \Omega \end{cases}$$

- Q is on $\partial\Omega_{FS}$,

$$\alpha\Phi - \int_{\partial\Omega_F} \Phi(P) \frac{\partial G}{\partial n}(P, Q) ds + \int_{\partial\Omega_B} \frac{\partial\Phi}{\partial n}(P) G(P, Q) ds =$$

$$\int_{\partial\Omega_B} \Phi(P) \frac{\partial G}{\partial n}(P, Q) ds - \int_{\partial\Omega_F} \frac{\partial\Phi}{\partial n}(P) G(P, Q) ds$$

- Q is on $\partial\Omega_{SB}$,

$$\int_{\partial\Omega_F} \Phi(P) \frac{\partial G}{\partial n}(P, Q) ds + \int_{\partial\Omega_B} \frac{\partial\Phi}{\partial n}(P) G(P, Q) ds =$$

$$\alpha\Phi + \int_{\partial\Omega_B} \Phi(P) \frac{\partial G}{\partial n}(P, Q) ds - \int_{\partial\Omega_F} \frac{\partial\Phi}{\partial n}(P) G(P, Q) ds.$$

- Φ and $\partial\Phi/\partial n$ known on $\partial\Omega_{FS}$ and $\partial\Omega_{SB}$ respectively
- Φ and $\partial\Phi/\partial n$ unknown on $\partial\Omega_{SB}$ and $\partial\Omega_{FS}$ respectively

Free surface $\Rightarrow N_{FS}$ panels, s_j , and solid boundaries $\Rightarrow N_{SB}$ panels

$$\alpha_i \Phi_i - \sum_{j=1}^{N_F} \int_{s_j} \Phi_j \frac{\partial G}{\partial n}(i, j) ds + \sum_{j=1}^{N_B} \int_{s_j} \frac{\partial \Phi_j}{\partial n} G(i, j) ds =$$

$$\sum_{j=1}^{N_F} \int_{s_j} \frac{\partial \Phi_j}{\partial n} G(i, j) ds + \sum_{j=1}^{N_B} \int_{s_j} \Phi_j \frac{\partial G}{\partial n}(i, j) ds,$$

where $1 < i < N_F + 1$ corresponds to the i^{th} point of FS ,

$$\sum_{j=1}^{N_F} \int_{s_j} \Phi_j \frac{\partial G}{\partial n}(i, j) ds + \sum_{j=1}^{N_B} \int_{s_j} \frac{\partial \Phi_j}{\partial n} G(i, j) ds =$$

$$\alpha_i \Phi_i + \sum_{j=1}^{N_F} \int_{s_j} \frac{\partial \Phi_j}{\partial n} G(i, j) ds - \sum_{j=1}^{N_B} \int_{s_j} \Phi_j \frac{\partial G}{\partial n}(i, j) ds,$$

where $1 < i < N_B + 1$ corresponds to the i^{th} point of SB .

The Green Green function is

$$G(P, Q) = \ln(|\mathbf{PQ}|). \quad (26)$$

or

$$G(P, Q) = \ln(\sqrt{\xi^2 + \vartheta^2}). \quad (27)$$

where (ξ, ϑ) are the coordinates of the vector \mathbf{PQ}

Hence

$$\frac{\partial G}{\partial n}(P, Q) = \frac{\vartheta}{\xi^2 + \vartheta^2}. \quad (28)$$

Φ et $\partial\Phi/\partial n$ are assumed to vary linearly along the panels

For points i on the free surface

$$\begin{aligned} \alpha_i \Phi_i - \sum_{j=1}^{N_F} \left\{ \Phi_{j+1} \frac{l_4 - \xi_j l_2}{\xi_{j+1} - \xi_j} + \Phi_j \frac{l_2 \xi_{j+1} - l_4}{\xi_{j+1} - \xi_j} \right\} + \\ \sum_{j=1}^{N_B} \left\{ \psi_{j+1} \frac{l_3 - \xi_j l_1}{\xi_{j+1} - \xi_j} + \psi_j \frac{l_1 \xi_{j+1} - l_3}{\xi_{j+1} - \xi_j} \right\} = \\ \sum_{j=1}^{N_F} \left\{ \psi_{j+1} \frac{l_3 - \xi_j l_1}{\xi_{j+1} - \xi_j} + \psi_j \frac{l_1 \xi_{j+1} - l_3}{\xi_{j+1} - \xi_j} \right\} + \\ \sum_{j=1}^{N_B} \left\{ \Phi_{j+1} \frac{l_4 - \xi_j l_2}{\xi_{j+1} - \xi_j} + \Phi_j \frac{l_2 \xi_{j+1} - l_4}{\xi_{j+1} - \xi_j} \right\} \end{aligned}$$

For points i on solid boundaries

$$\begin{aligned}
 & \sum_{j=1}^{N_F} \left\{ \Phi_{j+1} \frac{l_4 - \xi_j l_2}{\xi_{j+1} - \xi_j} + \Phi_j \frac{l_2 \xi_{j+1} - l_4}{\xi_{j+1} - \xi_j} \right\} + \\
 & \sum_{j=1}^{N_B} \left\{ \Psi_{j+1} \frac{l_3 - \xi_j l_1}{\xi_{j+1} - \xi_j} + \Psi_j \frac{l_1 \xi_{j+1} - l_3}{\xi_{j+1} - \xi_j} \right\} = \\
 & \alpha_i \Phi_i + \sum_{j=1}^{N_F} \left\{ \Psi_{j+1} \frac{l_3 - \xi_j l_1}{\xi_{j+1} - \xi_j} + \Psi_j \frac{l_1 \xi_{j+1} - l_3}{\xi_{j+1} - \xi_j} \right\} - \\
 & \sum_{j=1}^{N_B} \left\{ \Phi_{j+1} \frac{l_4 - \xi_j l_2}{\xi_{j+1} - \xi_j} + \Phi_j \frac{l_2 \xi_{j+1} - l_4}{\xi_{j+1} - \xi_j} \right\}
 \end{aligned}$$

Ψ corresponds to the normal derivative of the potential $\partial\Phi/\partial n$.

$$I_1 = \int_{\xi_1}^{\xi_2} \ln(\sqrt{x^2 + \vartheta^2}) dx$$

$$= \frac{1}{2} \xi_2 \ln(\xi_2^2 + \vartheta^2) - \xi_2 + \vartheta \arctan\left(\frac{\xi_2}{\vartheta}\right) - \frac{1}{2} \xi_1 \ln(\xi_1^2 + \vartheta^2) + \xi_1 - \vartheta \arctan\left(\frac{\xi_1}{\vartheta}\right)$$

$$I_2 = \int_{\xi_1}^{\xi_2} \frac{\vartheta}{x^2 + \vartheta^2} dx = \arctan\left(\frac{\xi_2}{\vartheta}\right) - \arctan\left(\frac{\xi_1}{\vartheta}\right)$$

$$I_3 = \int_{\xi_1}^{\xi_2} x \ln(\sqrt{x^2 + \vartheta^2}) dx$$

$$= \frac{1}{4} \xi_2^2 \ln(\xi_2^2 + \vartheta^2) + \frac{1}{4} \vartheta^2 \ln(\xi_2^2 + \vartheta^2) - \frac{1}{4} \xi_2^2 - \frac{1}{4} \xi_1^2 \ln(\xi_1^2 + \vartheta^2) - \frac{1}{4} \vartheta^2 \ln(\xi_1^2 + \vartheta^2) + \frac{1}{4} \xi_1^2$$

$$I_4 = \int_{\xi_1}^{\xi_2} \frac{x\vartheta}{x^2 + \vartheta^2} dx = \frac{1}{2}\vartheta \ln(\xi_2^2 + \vartheta^2) - \frac{1}{2}\vartheta \ln(\xi_1^2 + \vartheta^2)$$

- ▶ On solid boundaries ($\partial\Omega_{SB}$)

$$\nabla\Phi \cdot \mathbf{n} = \mathbf{v} \cdot \mathbf{n} \quad (29)$$

- ▶ On the free surface ($\partial\Omega_{FS}$)

$$\frac{d\mathbf{r}}{dt} = \nabla\Phi \quad (30)$$

$$\frac{d\Phi}{dt} = \frac{1}{2}(\nabla\Phi)^2 - g\eta - \frac{p_a}{\rho_w} \quad (31)$$

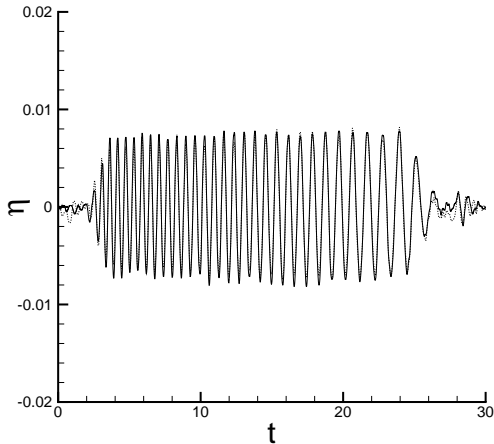
- ▶ Time stepping: A 4th-order Runge-Kutta scheme for the time marching of the free surface

In deep water

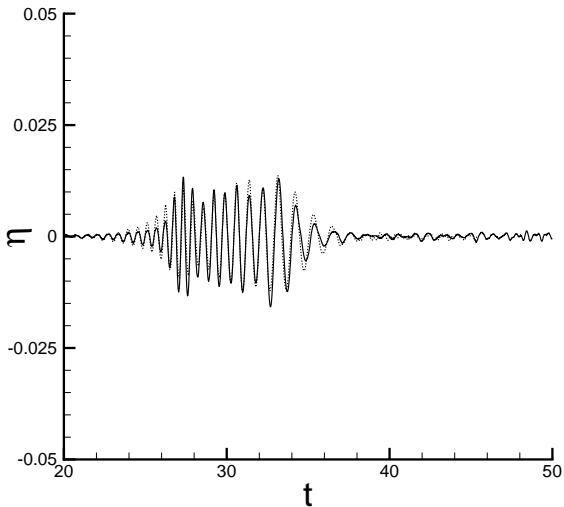
- ▶ Tank size: $L = 40m$ and $d = 1m$ ($N_{FS} = 1300$, $N_w = 700$)
- ▶ $\Delta t = 10^{-2} s$

Validation and simulations

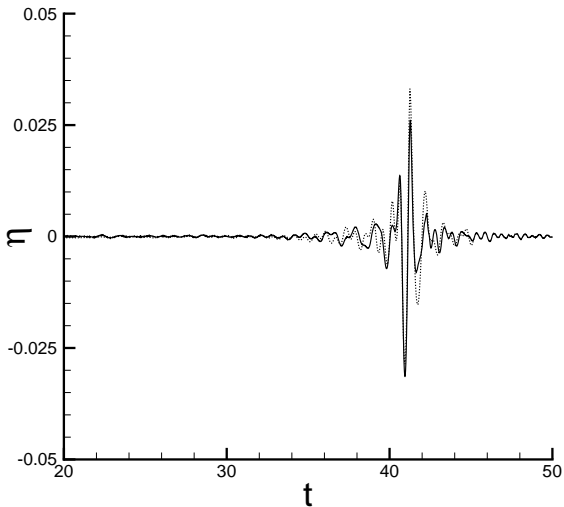
1.85Hz-0.75Hz in $T = 25s$



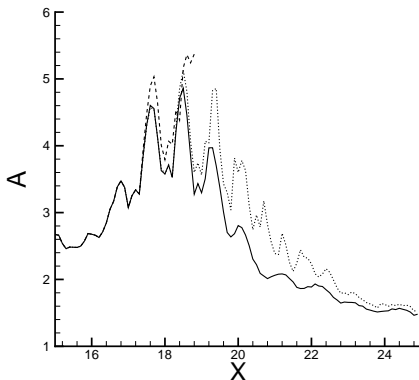
Experiments (solid lines) and numerical (dotted lines) surface elevations at fetch 1m



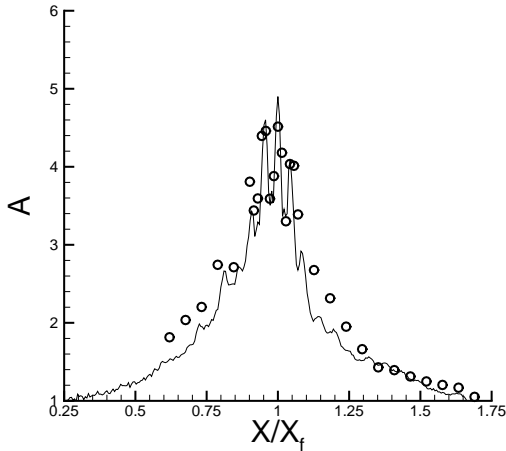
Experiments (solid lines) and numerical (dotted lines) surface elevations at fetch 11m



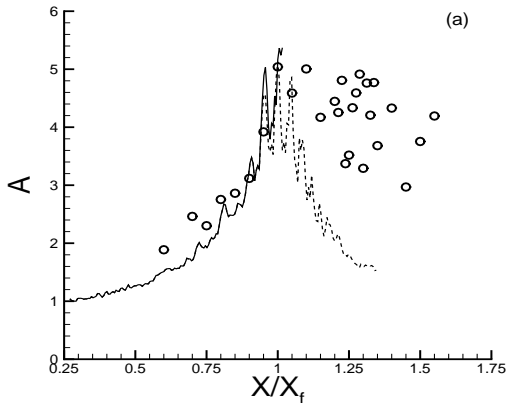
Experiments (solid lines) and numerical (dotted lines) surface elevations at fetch 18m



Numerical amplification factor $A(X, U)$ as a function of the distance (in m) for two values of the wind velocity within the framework of the dispersive focusing: $U = 0m/s$ (solid line), $U = 6m/s$ and $(\partial\eta/\partial x)_c = 0.4$ (dotted line), $U = 6m/s$ and $(\partial\eta/\partial x)_c = 0.3$ (dashed line)



Numerical (solid line) and experimental (circle) amplification factor $A(X/X_f, U)$ as a function of the normalized distance without wind ($U = 0$) within the framework of the dispersive focusing



(a) Numerical (solid and dashed lines) and experimental (circle) amplification factor $A(X/X_f, U)$ as a function of the normalized distance with wind ($U = 6\text{ m/s}$) for $(\partial\eta/\partial x)_c = 0.3$ (solid line) and $(\partial\eta/\partial x)_c = 0.4$ (dashed line) within the framework of the dispersive focusing



◀ ◻ ▶ ◀ ◻ ▶ ◀ ≡ ▶ ◀ ≡ ▶ ≡

Conclusions on numerical simulations in deep water

- ▶ The numerical simulations and experimental results are in qualitative agreement
- ▶ During the occurrence of extreme wave events the wind-driven current could play a significant role in their persistence

In shallow water

Generation of steep waves

- *Dispersive focusing*

Based on a linear approach of the problem

$$\frac{\partial \omega}{\partial t} + C_g \frac{\partial \omega}{\partial x} = 0$$

or equivalently

$$\frac{d\omega}{dt} = 0 \quad \text{along} \quad \frac{dx}{dt} = C_g(\omega)$$

where $d/dt = \partial/\partial t + C_g \partial/\partial x$

► *Inverse KdV method*

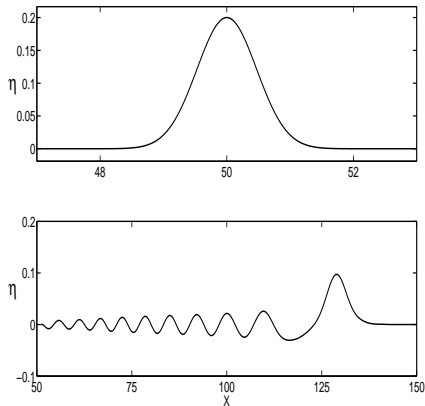


Fig. 2. Transformation of an initial Gaussian impulse (top) into soliton and dispersive wave train (bottom) within the framework of the KdV equation (η and x are given in m)

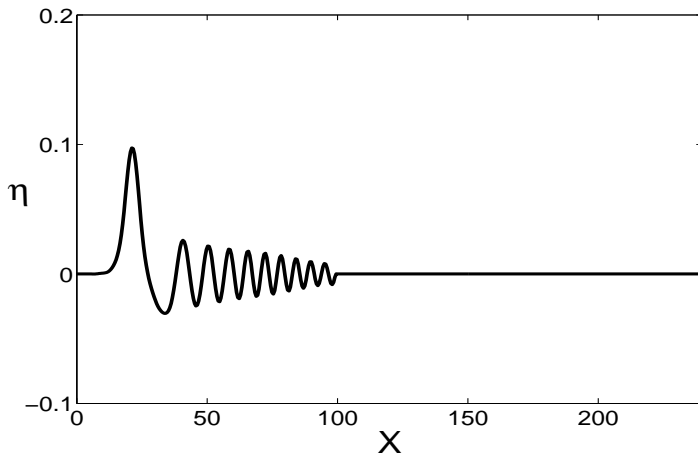


Fig. 3. Initial surface elevation from KdV equation (η and x are given in m)

Validation of the BIEM

Comparison between numerical simulation and experimental data without wind on the propagation of a breaking wave.

► *Experiments*

Wave tank of Ecole Centrale de Marseille: 17 m long, 0.65 m wide and 0.35 m deep, equipped of a flap-type wavemaker.

Large amplitude wave generation from focusing corresponding to the following Ricker spectrum

$$R(\omega) = A_r \sqrt{\pi} T_r e^{-\omega^2 T_r^2 / 4} \left(1 - a_r \left(\frac{1}{4} \omega^2 T_r^2 - \frac{1}{2} \right) \right)$$

$A_r = 0.1$ m amplitude of the steep wave event, $a_r = -0.7$ and $T_r = 0.23$ parameters to adjust peak pulsation and signal narrowness \Rightarrow focusing at 7.75 m

► *Numerical simulation*

Simulation of the ECM wave tank with the same conditions

Total number of meshes: 1100 with 660 on the free surface

Time step: 10^{-4}

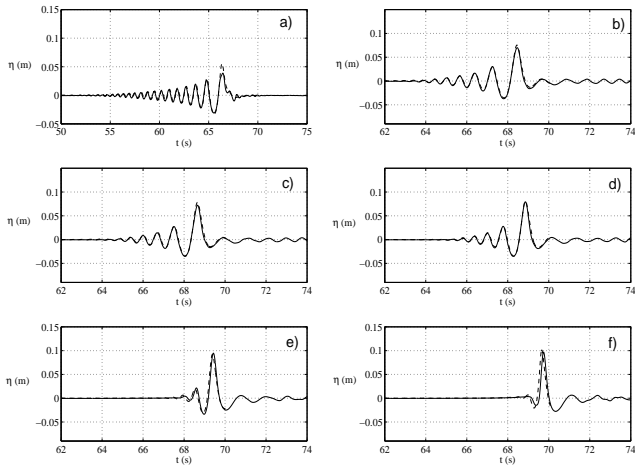


Fig. 4. Experiment (solid line); simulation (dashed line) : (a) $x = 1,7 m$, (b) $x = 5.37 m$, (c) $x = 5.73 m$, (d) $x = 6.09 m$, (e) $x = 7 m$ and (f) $x = 7.46 m$.

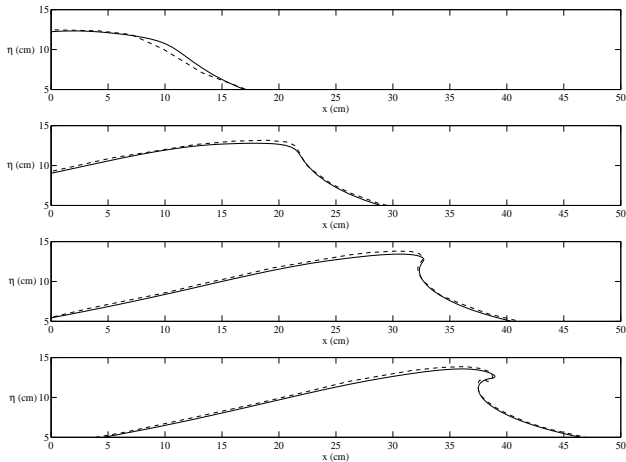


Fig. 5. Breaking wave: comparison between experimental data (dashed line) and numerical results (BIEM) without surface tension and viscosity (solid line). From top to bottom: $t = 2.19 \text{ s}$, $t = 2.27 \text{ s}$, $t = 2.34 \text{ s}$, $t = 2.37 \text{ s}$.

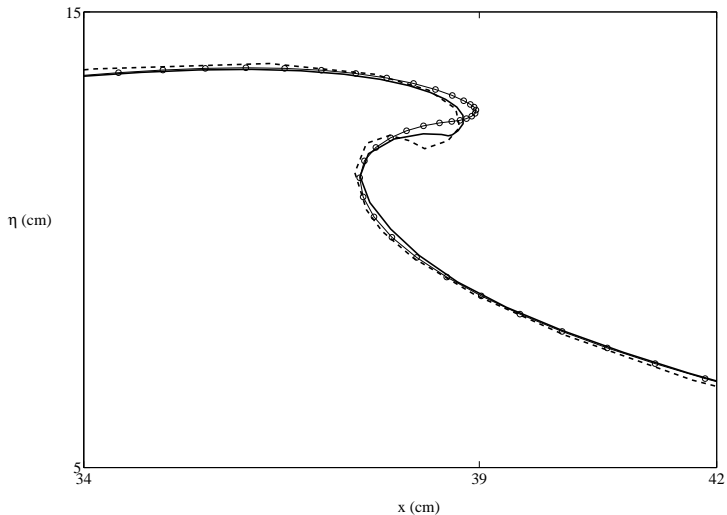


Fig. 6. Experimental data (dashed line) and numerical results (BIEM) with surface tension and viscosity (solid line), and without surface tension and viscosity (open circles).

Steep wave events in the presence of wind

- ▶ How do steep wave events due to dispersive focusing under wind action evolve?
- ▶ How are the amplification and time duration of these waves under wind effect modified?
- ▶ Are these effects similar or different from those observed in the case of extreme wave events due to spatio-temporal focusing in deep water?

Dispersive focusing

Equation of the piston type wavemaker is given by

$$s(t) = A \sin[\omega(t)t]$$

- ▶ $A = 0.05 \text{ m}$
- ▶ $0.5 < kh < 1$
- ▶ Length of the tank: 400 m
- ▶ Depth of the tank: 1 m
- ▶ Total number of meshes: 2000 with 1200 on the free surface
- ▶ Time step: 0.05 s

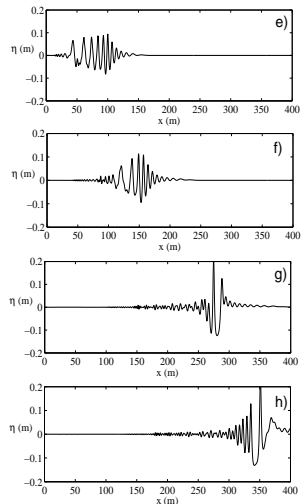
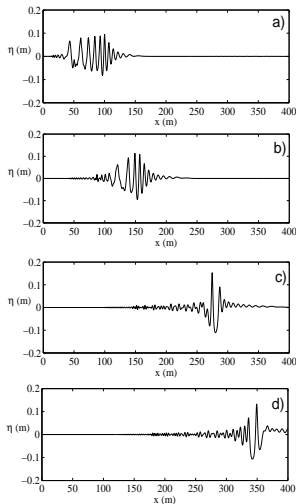


Fig. 7. Focusing wave train. *Without wind*: (a): $t = 50 \text{ s}$, (b): $t = 75 \text{ s}$, (c): $t = 125 \text{ s}$, (d): $t = 150 \text{ s}$. *With wind*, $U = 20 \text{ m.s}^{-1}$ and $(\partial\eta/\partial x)_c = 0.11$: (e): $t = 50 \text{ s}$, (f): $t = 75 \text{ s}$, (g): $t = 125 \text{ s}$, (h): $t = 150 \text{ s}$.

Let us define the amplification factor of the group of waves between initial time and time t as follows

$$A(t, U) = \frac{\eta_{\max}(t, U)}{\eta_{\text{ref}}}$$

η_{ref} : maximal wave amplitude at $t = 0$

$\eta_{\max}(t, U)$: maximal wave amplitude at t

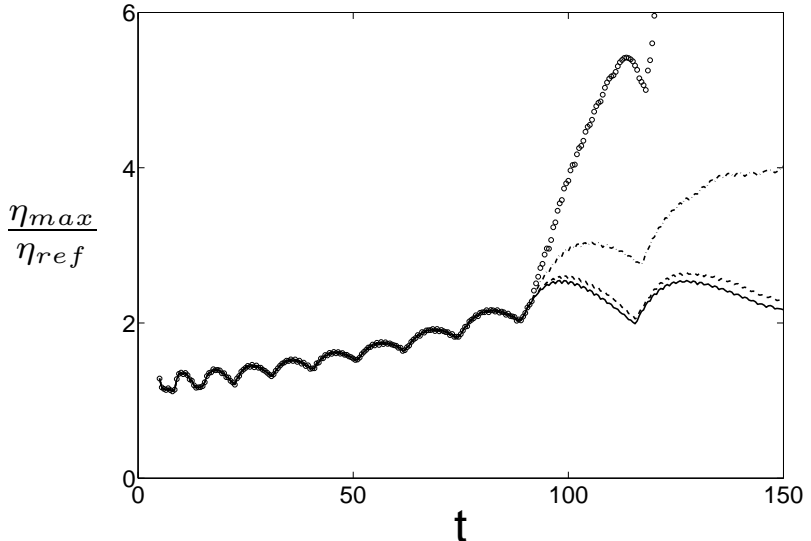


Fig. 8. Amplification factor $A(t, U)$ for several values of the wind speed: $U = 0 \text{ m} \cdot \text{s}^{-1}$ (solid line), $U = 10 \text{ m} \cdot \text{s}^{-1}$ (dashed line), $U = 20 \text{ m} \cdot \text{s}^{-1}$ (dot-dashed line), $U = 30 \text{ m} \cdot \text{s}^{-1}$ (open circle).

Inverse KdV method

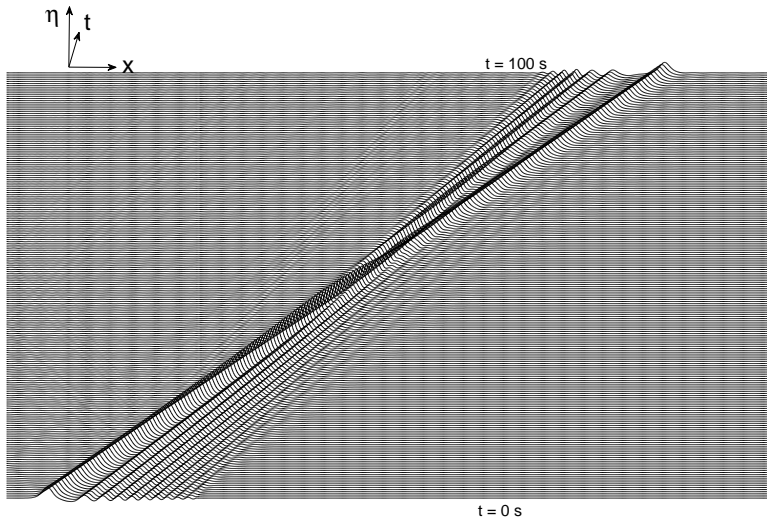


Fig. 9. Spatio-temporal evolution of the focusing and defocusing wave group in the absence of wind.

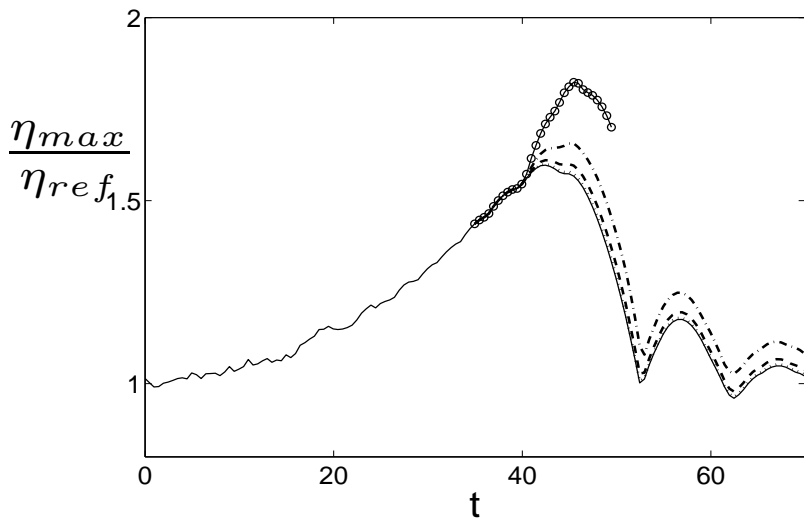


Fig. 10. Amplification factor $A(t, U)$ for several values of the wind speed: $U = 0 \text{ m} \cdot \text{s}^{-1}$ (solid line), $U = 8 \text{ m} \cdot \text{s}^{-1}$ (dotted line), $U = 16 \text{ m} \cdot \text{s}^{-1}$ (dashed line), $U = 20 \text{ m} \cdot \text{s}^{-1}$ (dot-dashed line), $U = 30 \text{ m} \cdot \text{s}^{-1}$ (open circle).

Wind effect on breaking wave phenomenon

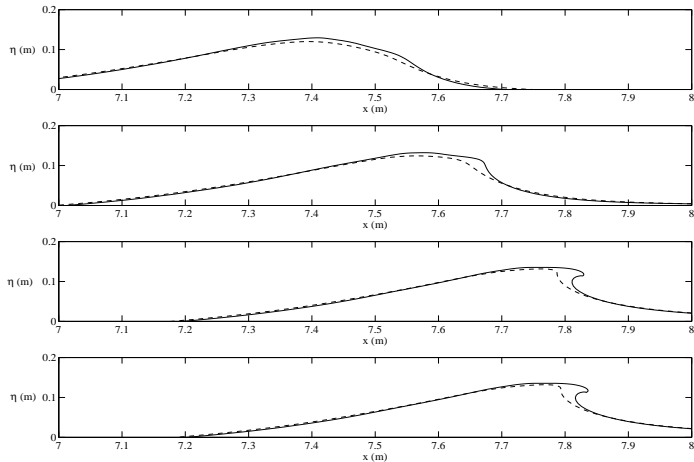


Fig. 11. Evolution of a breaking wave *with wind* (solid line) and *without wind* (dashed line). $U = 10 \text{ m} \cdot \text{s}^{-1}$ and $(\partial\eta/\partial x)_c = 0.20$.

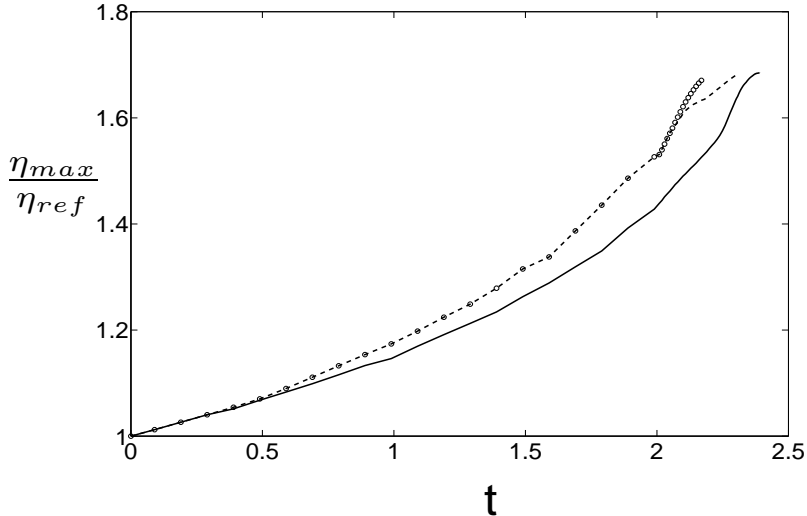


Fig. 12 Amplification factor $A(t, U)$ for a focusing wavetrain generated from a Ricker spectrum. *Without wind* (solid line), *with wind* $U = 10 \text{ m} \cdot \text{s}^{-1}$, $0.20 \leq \partial\eta/\partial x \leq \tan(\pi/6)$ (dashed line) and *with wind* $U = 10 \text{ m} \cdot \text{s}^{-1}$, $0.20 \leq \partial\eta/\partial x$ (open circles).

Conclusions on numerical simulation in shallow water

- ▶ Wind effect: (i) it increases the amplitude and lifetime of the highest waves in the group, (ii) it moves downwind the area where steep wave events are formed
- ▶ Steep wave events are less unstable to wind perturbation in shallow water than in deep water (*i.e.* stronger wind velocities are required in shallow water to produce breaking waves)
- ▶ Wind speeds up the overturning of the crest
- ▶ For more details see Chambarel *et al*, EJM B/Fluids, 29, 2010

III. General conclusions and perspectives

The wind increases the lifetime and amplitude of SWE

- ▶ Improvement of the wind modelling (Miles + Jeffreys mechanisms, introduction of the turbulence in air flow, etc.)
- ▶ Modelling the dissipation due to breaking wave
- ▶ Extension to 3D flows